WSRC-RP--89-1395

DE92 010190

FLOW BOILING IN VERTICAL DOWN-FLOW

T. Dougherty, C. Fighetti, G. Reddy, B. Yang, T. Jafri
Columbia University
New York, NY

E. McAssey
Villanova University
Villanova, PA

Z. Qureshi
Westinghouse Savannah River Co.
Aiken, S.C.

ABSTRACT

An experimental program has been conducted to investigate the onset of Ledinegg instability in vertical down-flow. For three size uniformly heated test sections with L/D ratios from 100 to 150, the pressure drop under subcooled boiling conditions has been obtained for a wide range of operating parameters. The results are presented in non-dimensional forms which correlate the important variables and provide techniques for predicting the onset of flow instability.

INTRODUCTION

Flow boiling in vertical channels is important to nuclear reactors because the formation of vapor can affect the heat transfer rate from the channel surface and also because the presence of vapor can increase the channel pressure drop resulting in flow instability excursions. The present study was undertaken to investigate flow instability and heat transfer for application in which the flow direction was vertically downward. The overall program involves testing in both single tubes and annuli. The present paper presents results for the single tube geometry with a length to diameter ratio range of 100 to 150.

BACKGROUND

Vertical up-flow in a heated channel has been investigated by a number of researchers. Dormer and Bergles (1964) investigated the pressure drop in small tube diameter under sub-cooled boiling conditions. These experiments were conducted with a controlled flow system so that data was obtained well into the unstable region. These investigators correlated a large amount of data using the ratio of sub-cooled boiling pressure drop to the single phase pressure drop versus the ratio of the surface heat flux to the surface heat flux required to raise the bulk fluid temperature to saturation at the channel exit. Using these parameters, it was shown that the only remaining effect was geometry. The results were predominantly dependent upon the length to diameter ratio. The diameter had a small but measurable effect. Maulbetsch and Griffith (1966) studied flow instability in small diameter high L/D ratio channels. They determined that during parallel flow operation excursive flow instability occurred when the pressure drop versus mass flow curve (demand curve) reached a minimum. Using the Dormer-Bergles (1964) correlation, Maulbetsch and Griffith (1966) were able to predict the demand curve (channel pressure drop vs. flowrate) with reasonable accuracy.

Whittle and Forgan (1967) examined the pressure loss in rectangular and circular channels under sub-cooled boiling conditions. These investigators determined that for a given L/D ratio the minimum in the pressure drop versus flow-rate curve occurred at a fixed value of the ratio of the channel temperature rise to the inlet sub-cooling.

The present study was undertaken to obtain data describing flow instability and heat transfer as a function of various operating parameters. The onset of flow instability (OFI) is related to the onset of significant voiding; however, the formation of voids generally precedes the onset of flow instability. For a uniformly heated channel with fixed inlet subcooling and exit pressure, the process of void formation can be initiated by decreasing the flow-rate to the channel. The voids are initially formed at the channel exit and the process of voiding then proceeds upstream from the channel exit. In up-flow, the buoyant and the convective forces, which are acting in the same direction, combine to sweep the voids out of the channel before a significant pressure effect can occur. As the flow-rate continues to decrease, the point

of void formation moves further into the channel and the bubbles become larger and more numerous. Initially, the effect of the bubbles is to increase the effective roughness of the channel; however, as the process continues the presence of voids significantly increases the frictional head loss. Since the phenomenon is occurring in a sub-cooled liquid, the pressure in the channel begins to oscillate rapidly as bubbles are formed and then condense. In down-flow, the convective force and the buoyancy forces are in opposite direction. Failure to sweep the voids from the channel can have a significant effect upon the onset of flow instability.

The experimental program has the objective of obtaining the demand curve through the onset of flow instability for a circular tube in down-flow. The tubes were heated uniformly with a maximum heat flux capability of 3.155 MW/m^2. In addition to pressure data, wall temperature was also measured so that information on heat transfer coefficient and nucleate boiling could be obtained.

TEST APPARATUS

An isometric drawing of the test loop is presented in Figure 1. The working fluid is deionized and degassed water pressurized by a helium blanket. Flow is provided by a centrifugal pump capable of producing a flow-rate of .947 m^3/min at 483 KPa pressure differential. The discharge from the pump can go either to the test section or be bypassed to the accumulator or the mixer. The mixer is located downstream of the test section to eliminate any vapor before the mixture enters a plate type heat exchanger which removes energy from the loop. Control valves are provided to allow the adjustment of the flow-rate in each of these three paths.

The test section consists of a 2.44 m heated length. The tube material was either stainless steel 316 or inconel 600. Results will be presented for four different tube inside diameters (15.44 mm, 18.9 mm, 25.3 mm, and 28.6 mm). The wall thickness for all test sections was 1.65 mm. The section was mounted vertically with flow entering from the top. An entrance and exit length of approximately 18 diameters was provided. This section consisted of a copper tube with a wall thickness between 12.7 mm and 19.1 mm depending the test section inside diameter. Thermal input was supplied by passing a DC current through the tube wall. The exterior of the entire test

section was insulated with a layer of ceramic paper, 25.4 mm fiberglass rope, and 101 mm of Invisal insulation.

The test section and flow loop were instrumented with a number of sensors; however, the primary instrumentation consisted of the following.

1) 25.4 mm turbine flow-meters located upstream and downstream of the test section. These units were manufactured by the Hoffer Corporation and were calibrated over a range of 0 to .189 m^3/min to within +/- 0.189 $*10^{-3}$ m^3/min.

2) Test section pressure drop was measured by means of two differential pressure transducers (Sensotec) located 180 degrees apart and a mercury manometer. The pressure taps were located in the calming section approximately 57 mm upstream and downstream of the heated length. The pressure transducer was calibrated to within +/- 0.172 KPa.

3) Test section wall temperature was monitored by E type thermocouples mounted on the tube outside diameter. The thermocouples were located every 0.3048 m along the test section. At each axial location, two thermocouples were mounted 180 degrees apart. The circumferential orientation was rotated 90 degrees at each axial location.

4) The test section inlet and exit temperatures were monitored by RTD's which were calibrated with a complete bridge to within +/- 0.1 ^{o}C. These sensors were located in the elbows beyond the calming length.

5) The test section inlet and exit pressures were measured by Sensotec absolute pressure transducers which were calibrated to within +/- 1.38 KPa.

The test control parameters were the test section exit pressure, the test section inlet temperature, and the average thermal flux. Starting at a maximum test section flow-rate of .113 m^3/min to .151 m^3/min, the flow-rate was decreased and the pressure drop across the test section was recorded. The flow-rate was decreased until a minimum pressure loss was recorded. Several points beyond the minimum were also taken to insure an accurate OFI point. Prior to the instability point, the pressure reading were

steady; however, as the OFI point was reached, the pressure reading oscillated violently. After establishing OFI, the flow-rate was then increased and system returned to its initial condition. In this way, the demand curve was followed in both directions.

RESULTS AND DISCUSSION

The four different diameter test section were examined over a range of conditions. Table 1 presents the test section data for these tubes.

Table 1
Test Section of Configuration

Inside Diameter	Heated Length	Wall Thickness	Material
15.54 mm	2.44 m	1.65 mm	Inconel 600
18.92 mm	2.44 m	1.65 mm	Stainless 316
25.27 mm	2.44 m	1.65 mm	Stainless 316
28.6 mm	2.44 m	1.65 mm	Inconel

The test matrix used for each test section is given in Table 2.

Table 2
Test Matrix

Surface Heat Flux	Exit Pressure	Inlet Temperature
1.262 MW/m^2	137.9KPa, 344.8 KPa	25 ^oC, 50 ^oC
1.893 MW/m^2	137.9KPa, 344.8 KPa	25 ^oC, 50 ^oC
2.524 MW/m^2	137.9KPa, 344.8 KPa	25 ^oC, 50 ^oC
3.155 MW/m^2	137.9KPa, 344.8 KPa	25 ^oC, 50 ^oC

Figure 2 presents typical demand curves for the 15.54 mm diameter test section at a test section exit pressures of 344.75 KPa and inlet temperature of 25 ^oC. At high flow-rates, the demand curve follows a profile typical of single phase. Calculations have shown that the results follow the Darcy formula very well; however, as the flow-rate decreases, voids begin to form and the profile deviates from the velocity squared relationship. Lowering the system exit saturation temperature increases void production for a given flux and thereby causes flow instability to begin at a higher flow-rates. Increasing the inlet temperature has a similar effect

because it reduces the temperature difference between the saturation temperature and the fluid bulk temperature.

Dormer and Bergles (1964) noted that the ratio of surface heat flux to the flux required to heat the fluid from the inlet temperature to the saturation temperature could be used as a correlating parameter. The flux to saturation involves the flowrate, inlet temperature, and exit pressure (saturation temperature). Figures 3, 4, and 5 present the pressure versus the flux/flux to saturation ratio (q''/q''_{sat}) for three different size tube and various operating conditions. The single phase region corresponding to high flowrate is represented by small values of the ratio. As the ratio is increased each figure shows the pressure going through a minimum point. This point corresponds to the onset of flow instability (OFI). The OFI point for each size tube occurs at approximately the same value of the flux / flux to saturation ratio independent of surface heat flux, inlet temperature and operating pressure. This is in agreement with the observations of Whittle and Forgan (1967). Figure 6 present the value of the q''/q''_{sat} at OFI versus the channel L/D ratio. The data spread for all test sections is less than 5%.

Figure 7 presents the wall superheat (wall surface temperature - saturation temperature) versus q''/q''_{sat} for various distances along the channel. For a q''/q''_{sat} ratio greater than 0.7, the wall superheat is constant for x/l of 0.1 or less. This effect is related to the onset of nucleate boiling. For a uniformly heated channel, ONB begins at the channel exit and proceeds into the channel. From figure 7, it appears that ONB has not reached the point where $x/l = 0.25$. Figure 8 presents a similar plot showing the effect of surface heat flux at a fixed channel position. At heat fluxes of 2.524 MW/m^2 and 3.155 MW/m^2, nucleate boiling has occurred; however, at the lowest flux the flowrate is apparently sufficiently large enough to prevent nucleate boiling. Under nucleate boiling conditions, the wall superheat is independent of flux. Figure 9 shows the effect of exit pressure for the larger fluxes. Decreasing the exit pressure increases the wall superheat under nucleate boiling conditions. At an exit pressure of 345 KPa, ONB occurs at a wall superheat of 28 ^{o}C, lowering the pressure to 138 PKa increases the superheat to 31 ^{o}C.

Using the calculated wall surface temperature and local fluid temperature, the heat transfer coefficient at various axial

locations can be determined. Figure 10 presents the heat transfer coefficient versus the flux ratio as a function of distance from the channel exit. As the flux ratio increases, the heat transfer coefficient decreases due to the drop in fluid velocity. At a q''/q''_{sat} ratio of approximately 0.6, the coefficient at $x/l = 0.04$ and 0.1 rise steeply. This reflects the onset of nucleate boiling and agrees with the results in figure 7. At $x/l = 0.25$, there is a slight increase in heat transfer coefficient but the change is considerably less than that $x/l = 0.04$ and 0.1. Figure 11 presents the variation as a function of surface heat flux. In this figure, the minimum in the heat transfer coefficient occurs at the same flux ratio. Because of space limitations, results for other size tubes have not been presented; however, analysis for these tubes indicates similar trends. In general, the onset of nucleate boiling occurs at flowrates 20% to 25% higher than the OFI flowrate. At OFI, the nucleate boiling region has propagated approximately 10 to 15 tube diameters into the test section.

CONCLUSIONS

Based upon the data obtained in this study, the following observations regarding the onset of flow instability and nucleate boiling can be made:

1) the demand curve clearly shows the onset of flow instability.

2) the flux ratio (q''/q''_{sat}) can be used to correlate various flow and operating conditions

3) the OFI point is strongly dependent upon the L/D ratio and can be predicted by the ratio of q''/q''_{sat}.

4) both wall superheat and heat transfer coefficient results indicate the onset of nucleate boiling.

5) although occurring a lower flowrate the ONB point flows an L/D ratio trend similar to the OFI point.

The current test program is continuing with the expansion of the test section L/D range. In addition, tests will be conducted on non-uniformly heated test sections. Steady state and transient tests will also be performed on a large L/D annular test section.

ACKNOWLEDGEMENT

Funding for this program was provided by the Savannah River Laboratory under Westinghous Savannah River Co. Contract AX-721092. The authors wish to express their appreciation to their colleagues at Columbia University's Heat Transfer Research Facility for their assistance in the design, construction, and operation of the experimental facility.

REFERENCES

Dormer, J. Jr. and Bergles, A.E., 1964, "Pressure Drop with Surface Boiling in Small Diameter Tubes, Report no. 8767-31, Dept. of Mech. Engng. MIT.

Maulbetsch, J.S. and Griffith, P., 1966, "System Induced Instabilities in Forced-Convective Flows with Sub-cooled Boiling", Proc. of the Third Int. Heat Transfer Conf., p 247-257.

Whittle, R.H. and Forgan, R., 1967, "A Correlation for the Minima in the Pressure Drop Versus Flow-rate Curves for Sub-cooled Water Flowing in Narrow Heated Channels", Nuclear Engineering and Design, Vol. 6, pp-89-99.

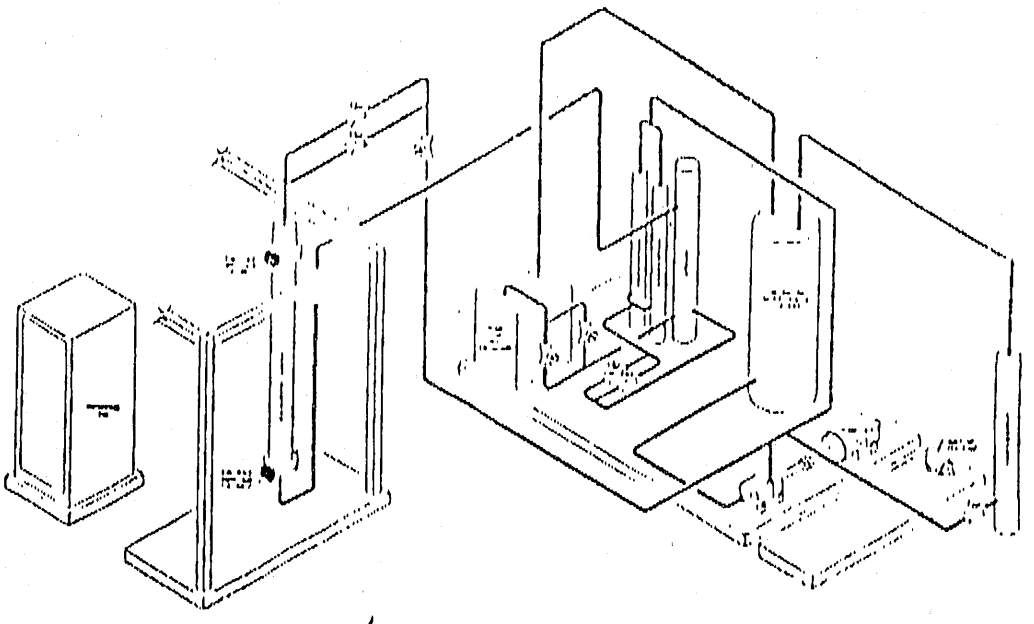

Figure 2 Isometric of test loop

Corporation and were calibrated over a range of 0 to .189 m^3/min to within +/- 0.189 $*10^{-3}$ m^3/min.

2) Test section pressure drop was measured by means of two differential pressure transducers (Sensotec) located 180 degrees apart and a mercury manometer. The pressure taps were located in the calming section approximately 57 mm upstream and downstream of the heated length. The pressure transducer was calibrated to within +/- 0.172 KPa.

3) Test section wall temperature was monitored by E type thermocouples mounted on the tube outside diameter. The thermocouples were located every 0.3048 m along the test section. At each axial location, two thermocouples were mounted 180 degrees apart. The circumferential orientation was rotated 90 degrees at each axial location.

4) The test section inlet and exit temperatures were monitored by RTD's, which were calibrated with a complete bridge to within +/- 0.1 ^{o}C. These sensors were located in the elbows beyond the calming length.

5) The test section inlet and exit pressures were measured by Sensotec absolute pressure transducers, which were calibrated to within +/- 1.38 KPa.

The test control parameters were the test section exit pressure, the test section inlet temperature, and the average thermal flux. Starting at a maximum test section flow-rate of .113 m^3/min to .151 m^3/min, the flow-rate was decreased and the pressure drop across the test section was recorded. The flow-rate was decreased until a minimum pressure loss was recorded. Several points beyond the minimum were also taken to insure an accurate OFI point. Prior to the instability point, the pressure readings were steady; however, as the OFI point was reached, the pressure reading oscillated violently. After establishing OFI, the flow-rate was then increased and system returned to its initial condition. In this way, the demand curve was followed in both directions.

RESULTS AND DISCUSSION

The three different diameter test sections were examined over a range of conditions. Table 1 presents the test section data for these tubes. The test matrix used for each test section is given in Table 2.

Figure 3 presents typical demand curves for the 15.54 mm diameter test section at a test section exit pressures of 344.75 KPa and inlet temperature of 25 ^{o}C. At high flow-rates, the demand curve follows a profile typical of single phase. Calculations have shown that the results follow the Darcy formula very well; however, as the flow-rate decreases, voids begin to form and the profile deviates from the velocity squared relationship.

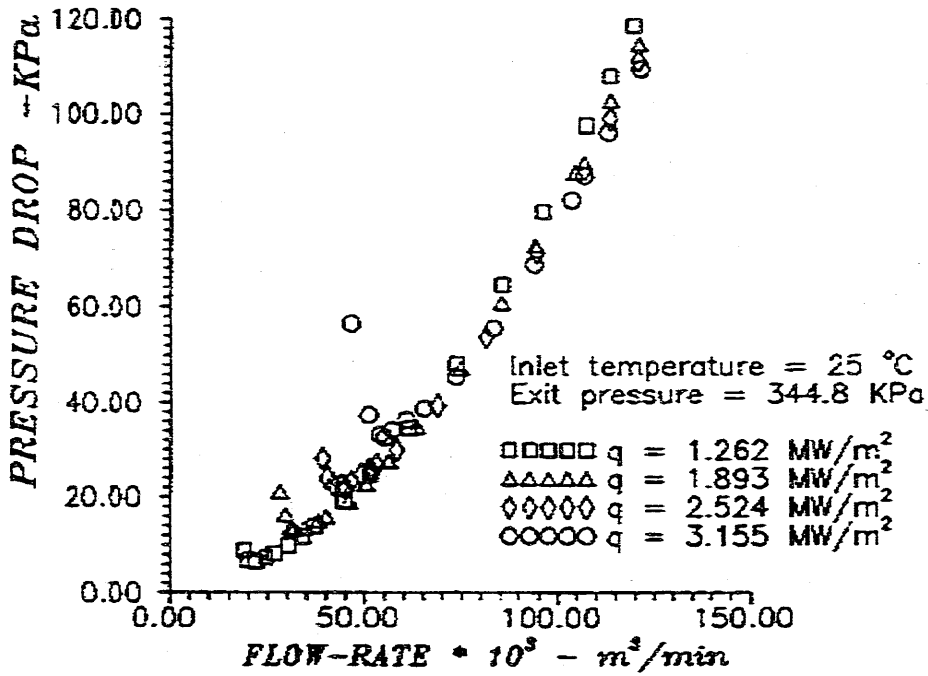

Figure 2 demand curve for 15.54 mm tube

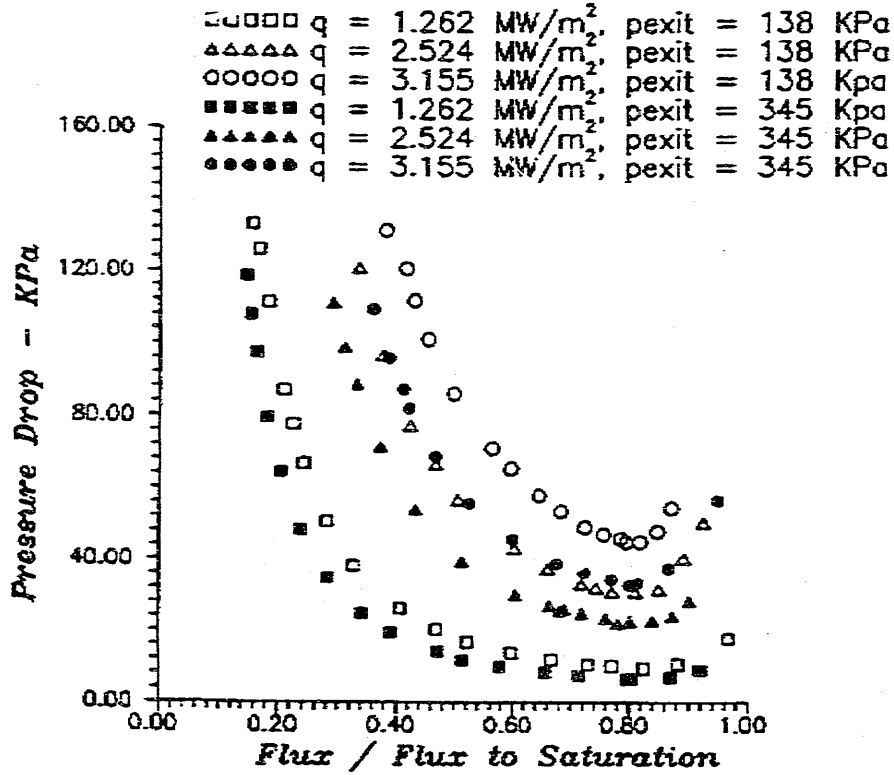

Figure 3 pressure drop versus flux/flux to saturation for a 15.5 mm diameter tube with inlet temperature = 25 °C

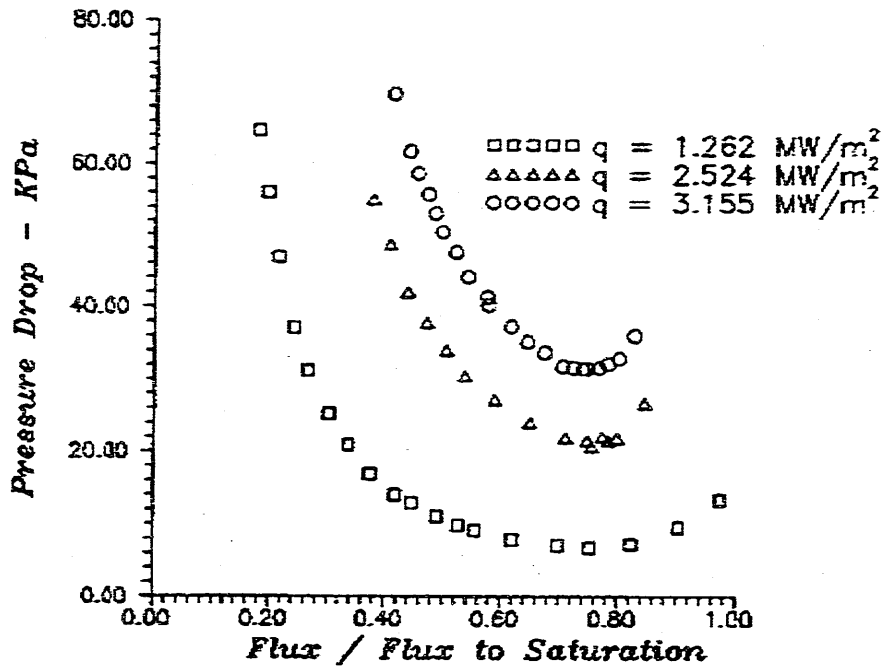

Figure 4 pressure drop versus flux/flux to saturation for a 18.8 mm diameter tube with exit pressure = 344.8 KPa and inlet temperature = 50 °C

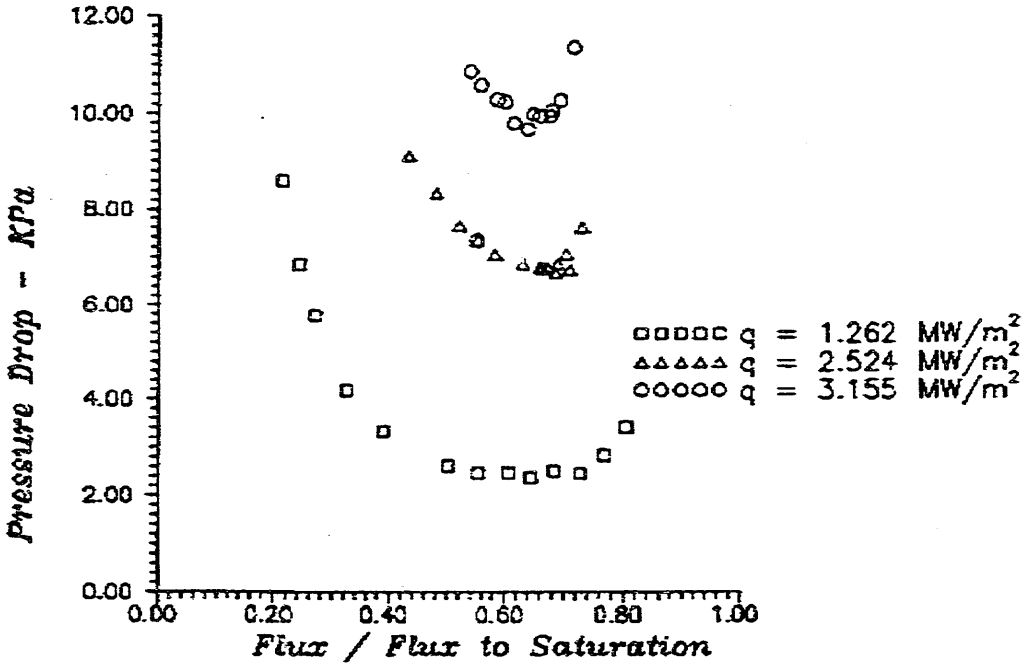

Figure 5 pressure drop versus flux/flux to saturation for a 28.6 mm diameter tube with exit pressure = 344.8 KPa and inlet temperature = 25 °C

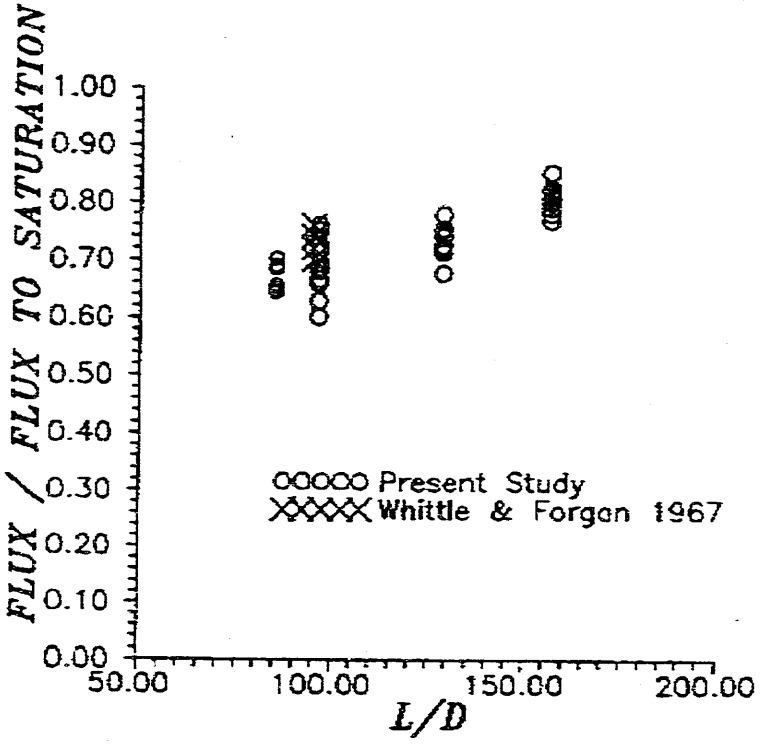

Figure 6 flux/flux to saturation at OFI vs. L/D ratio

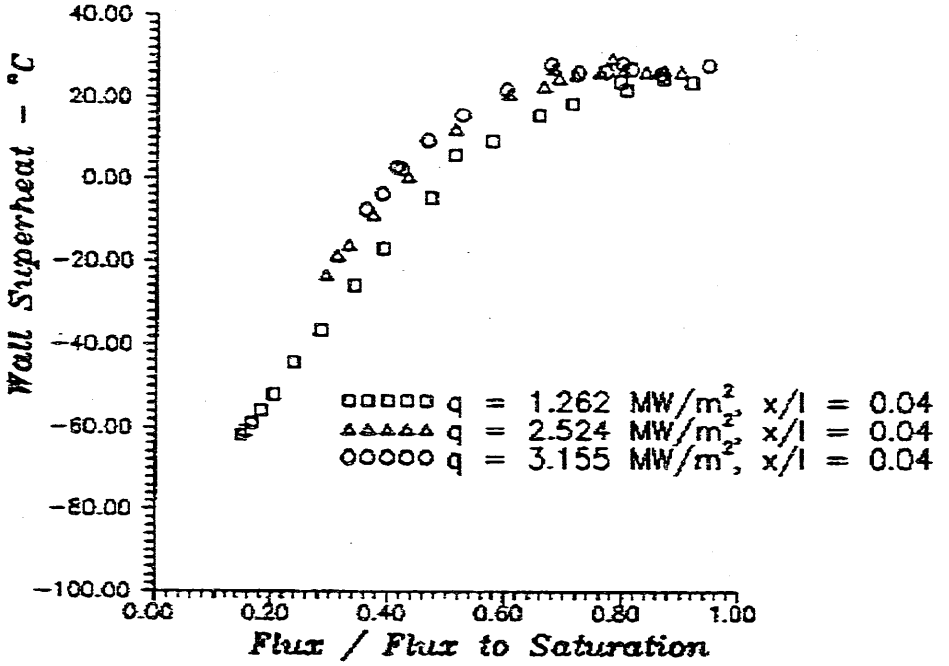

Figure 8 wall superheat vs. flux/flux to saturation for a 15.5 mm diameter tube with inlet temperature = 25 °C, and exit pressure = 344.8 KPa

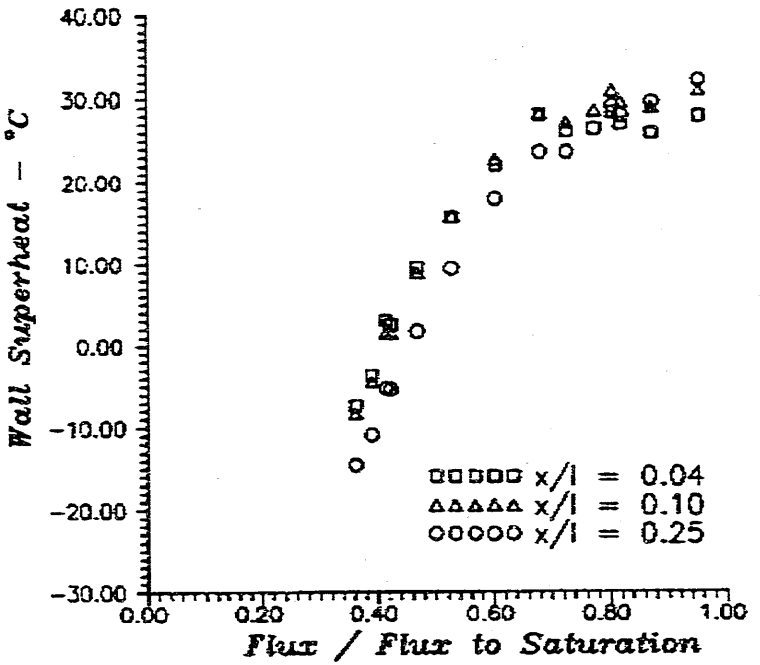

Figure 7 wall superheat vs. flux/flux to saturation for a 15.5 mm diameter tube with inlet temperature = 25 °C, exit pressure = 344.8 KPa, and surface heat flux = 3.155 MW/m.^{2}

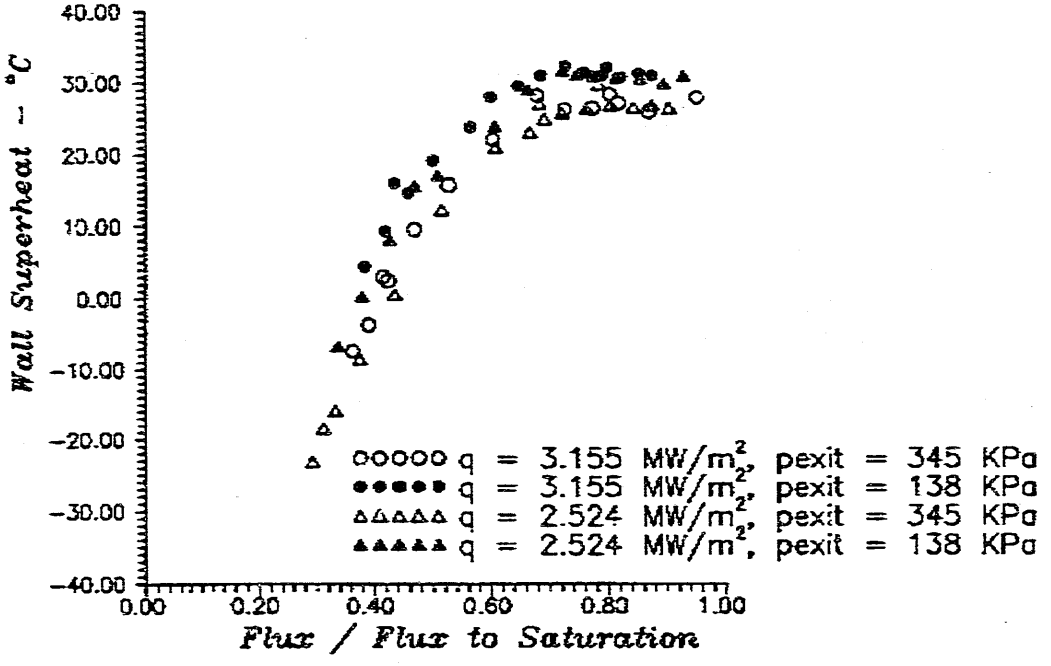

Figure 9 wall superheat vs. flux/flux to saturation for a 15.5 mm diameter tube with inlet temperature = 25 °C, and x/l = 0.04

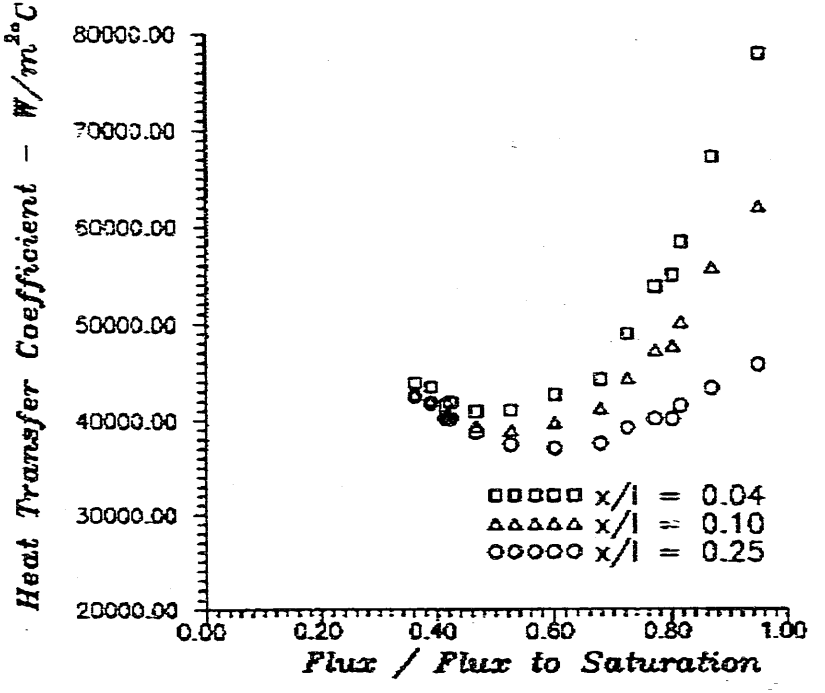

Figure 10 heat transfer coefficient vs flux/flux to saturation for a 15.5 mm diameter tube with inlet temperature = 25 °C, exit pressure = 344.8 KPa, and surface heat flux = 3.155 MW/m^2

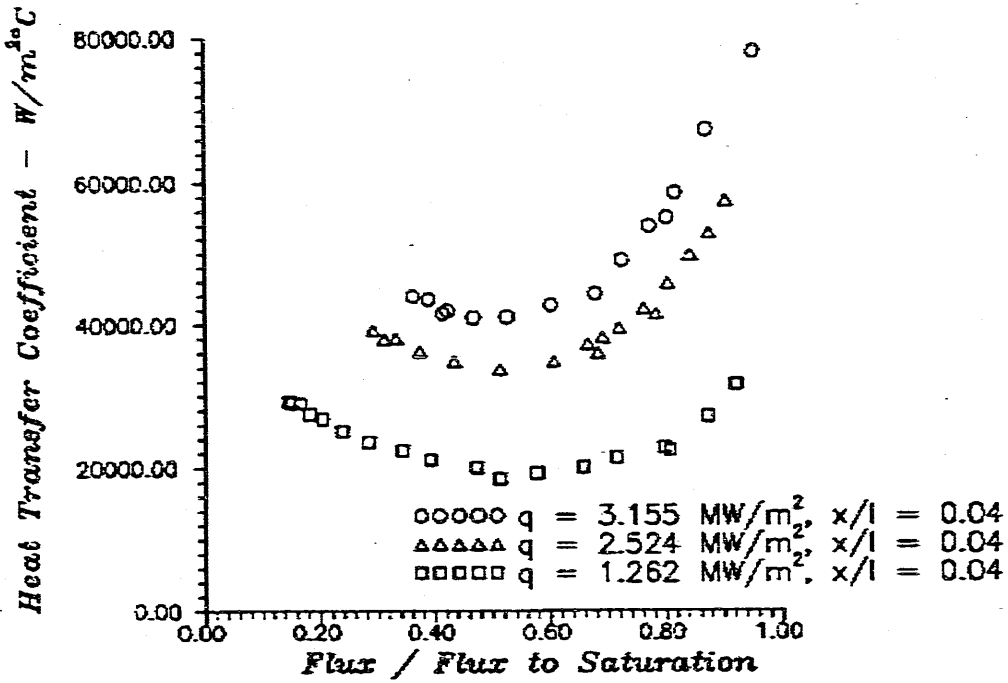

Figure 11 heat transfer coefficient vs. flux/flux to saturation for a 15.5 mm diameter tube with inlet temperature = 25 °C and exit pressure = 344.8 KPa

END

DATE
FILMED
4 129192